


RESEARCH ARTICLE

Open Access

Semaphorin 3A mediated brain tumor stem cell proliferation and invasion in EGFRviii mutant gliomas



Dominique M. O. Higgins^{1,2*} , Maisel Caliva^{3,4}, Mark Schroeder⁵, Brett Carlson⁵, Pavan S. Upadhyayula², Brian D. Milligan^{1,6}, Samuel H. Cheshier⁷, Irving L. Weissman⁸, Jann N. Sarkaria⁵, Fredric B. Meyer³ and John R. Henley³

Abstract

Background: Glioblastoma multiforme (GBM) is the most common primary brain tumor in adults, with a median survival of approximately 15 months. Semaphorin 3A (Sema3A), known for its axon guidance and antiangiogenic properties, has been implicated in GBM growth. We hypothesized that Sema3A directly inhibits brain tumor stem cell (BTSC) proliferation and drives invasion via Neuropilin 1 (Nrp1) and Plexin A1 (PlxnA1) receptors.

Methods: GBM BTSC cell lines were assayed by immunostaining and PCR for levels of Semaphorin 3A (Sema3A) and its receptors Nrp1 and PlxnA1. Quantitative BrdU, cell cycle and propidium iodide labeling assays were performed following exogenous Sema3A treatment. Quantitative functional 2-D and 3-D invasion assays along with shRNA lentiviral knockdown of Nrp1 and PlxnA1 are also shown. In vivo flank studies comparing tumor growth of knockdown versus control BTSCs were performed. Statistics were performed using GraphPad Prism v7.

Results: Immunostaining and PCR analysis revealed that BTSCs highly express Sema3A and its receptors Nrp1 and PlxnA1, with expression of Nrp1 in the CD133 positive BTSCs, and absence in differentiated tumor cells. Treatment with exogenous Sema3A in quantitative BrdU, cell cycle, and propidium iodide labeling assays demonstrated that Sema3A significantly inhibited BTSC proliferation without inducing cell death. Quantitative functional 2-D and 3-D invasion assays showed that treatment with Sema3A resulted in increased invasion. Using shRNA lentiviruses, knockdown of either NRP1 or PlxnA1 receptors abrogated Sema3A antiproliferative and pro-invasive effects. Interestingly, loss of the receptors mimicked Sema3A effects, inhibiting BTSC proliferation and driving invasion. Furthermore, in vivo studies comparing tumor growth of knockdown and control infected BTSCs implanted into the flanks of nude mice confirmed the decrease in proliferation with receptor KD.

Conclusions: These findings demonstrate the importance of Sema3A signaling in GBM BTSC proliferation and invasion, and its potential as a therapeutic target.

Keywords: Semaphorin, Neuropilin, Plexin, Glioma, Brain tumor stem cells

* Correspondence: dh2737@cumc.columbia.edu

¹Mayo Clinic: College of Medicine, Rochester, MN 55905, USA

²Department of Neurosurgery, Columbia University Medical Center, 710 W. 168th Street, New York, NY 10032, USA

Full list of author information is available at the end of the article



© The Author(s). 2020 **Open Access** This article is licensed under a Creative Commons Attribution 4.0 International License, which permits use, sharing, adaptation, distribution and reproduction in any medium or format, as long as you give appropriate credit to the original author(s) and the source, provide a link to the Creative Commons licence, and indicate if changes were made. The images or other third party material in this article are included in the article's Creative Commons licence, unless indicated otherwise in a credit line to the material. If material is not included in the article's Creative Commons licence and your intended use is not permitted by statutory regulation or exceeds the permitted use, you will need to obtain permission directly from the copyright holder. To view a copy of this licence, visit <http://creativecommons.org/licenses/by/4.0/>. The Creative Commons Public Domain Dedication waiver (<http://creativecommons.org/publicdomain/zero/1.0/>) applies to the data made available in this article, unless otherwise stated in a credit line to the data.

Background

Glioblastoma Multiforme (GBM) is a malignant glial brain tumor with a very poor prognosis [1–6]. One attribute responsible for the aggressiveness and refractory nature of these tumors is the presence of endogenous stem cell like GBM cells [7–11]. These subpopulations demonstrate increased resistance to chemotherapy and radiotherapy [12, 13]. Therefore, identification of novel therapeutics that target these brain tumor stem cell (BTSC) populations is essential to effectively treating this disease. In addition to its resistance to standard treatments, the extensive invasiveness of GBM also contributes to the lethality of this tumor [1, 14–17]. Despite attempted gross total resections by surgery, these tumors inevitably recur, as tumor cells can often be found well beyond the radiographically and surgically visible tumor boundary [18–24]. Indeed, a stereotypical feature of late stage GBM is the “butterfly pattern” of invasion, which is tumor cells migrating across the corpus callosum to the contralateral hemisphere [21, 25]. Further studies into invasive patterns of GBM have revealed a proclivity of GBM cells for migration along white matter tracts and blood vessels, known as secondary structures of Scherer [25]. Therefore, regulation of GBM invasion is at the core of successful treatment. Interestingly, these migratory patterns closely resemble those of normal neural stem and progenitor cells [26]. This indicates that BTSCs may be responding to endogenous guidance factors directing invasion.

One potential regulator of GBM stem cells is the guidance cue, Semaphorin 3A (Sema3A) [27–31]. Sema3A belongs to the Semaphorin family of proteins that are characterized by the presence of a 500 amino acid sema domain [32, 33]. Its cognate holoreceptor complex is comprised of Neuropilin-1 (Nrp1) and PlexinA1 (PlxnA1). Sema3A reportedly binds exclusively to Nrp1 [34–37]. In the absence of ligand, Nrp1 inhibits PlxnA1 intracellular signaling. Sema3A binding to Nrp1 results in a conformational change in the associated PlxnA1, leading to activation of a variety of downstream mediators [32, 37–42]. Sema3A has also been shown to have potent antiangiogenic effects, inhibiting endothelial cell proliferation and blood vessel formation [37, 43–46]. Classically, Sema3A is known for its effects on chemotaxis, especially in the nervous system [31]. Sema3A induces repulsion and collapse of certain axonal growth cones, but serves as an attractant for dendrites [30, 47–51]. This guidance cue is therefore uniquely poised to potentially differentially regulate cellular growth and migration. Prior studies have shown that inhibition of autocrine Sema3A can inhibit GBM invasion, and devascularize the tumors [52–55]. However, the direct role of exogenous Sema3A and its receptor complex in GBM stem cells has remained ill defined.

Objectives

In this study, we demonstrate that Sema3A inhibits proliferation, while stimulating invasion of BTSCs, in a Nrp1 and PlxnA1 dependent manner. Additionally, we propose a novel mechanism of action by Sema3A, where binding of the ligand to its receptors inhibits a constitutively “on” signal to drive proliferation and suppress invasion. We also highlight the potential role of Nrp1 as a marker of BTSCs. Taken together, the results presented here demonstrate the significance of the Sema3A signaling axis as a key regulator of GBM stem cells and therapeutic target.

Methods

Cell lines

GBM xenograft cell lines used are all established from tumor tissue harvested from patients undergoing surgical resection at the Mayo Clinic, Rochester, Minnesota. The studies were approved by the Mayo Clinic Institutional Review Board and necessary patient consents were obtained. All xenograft lines are from tumors classified as Grade IV gliomas based off of WHO Criteria. Cell lines are tested for mycoplasma infection prior to experiments and are routinely tested as part of maintenance protocols [56]. All cell lines used are mycoplasma free. Cell lines are available upon request from Dr. Sarkaria.

Cell sorting

Xenograft cells were labeled with microbeads conjugated to CD133 antibodies (Miltenyi), according to manufacturers’ specifications. Cells were then washed and applied to magnetic columns (Miltenyi). The flow through obtained was designated the CD133-low fraction. The column bound fraction was eluted and then sorted again to improve purity. This double sorted bound fraction was designated CD133-high. Fractions could then be analyzed by flow cytometry to assess and confirm enrichment of CD133.

Flow Cytometry

Cells were fixed on ice for 20 min with 2% paraformaldehyde, blocked with 10% NGS for 1 h, followed by primary antibody incubation with PE-conjugated CD133 (Miltenyi) for 30 min. Labeled cells were analyzed using a BD Calibur, with unlabeled cells serving as negative controls. For cell cycle analysis, cells were pre-treated for 24 h with 100 ng/mL Sema3A, dissociated, and fixed with cold 70% ethanol for 30 min at 4 °C. Cells were washed and treated with RNase (Qiagen). Propidium Iodide (PI) was added to the cells and analysis was conducted using a BD Calibur, with post-analysis using FlowJo software version 7.6.5.

GBM stem cell culture

All animal studies were approved by the Mayo Clinic Institutional Animal Care and Use Committee. All experiments were performed in compliance with and according to guidelines by the National Institutes of Health (NIH, Bethesda, MD, USA) and the Mayo Clinic (Rochester, MN, USA) Institutional Review Board and Institutional Animal Care and Use Committee guidelines as previously described in Carlson et al. [57]. Established xenograft tumors were harvested from the flanks of athymic nude mice (athymic nude- *foxn1nu*) (Harlan). Briefly, primary human GBM samples were directly implanted into the flank of 6–8 week old athymic nude-*foxn1^{nu}* mice in a 1:1 ratio by volume of tumor and Matrigel (Fisher). Tumors were aseptically dissected away from mouse flanks, and dissociated mechanically, then enzymatically with papain. Tumor cells were plated in stem cell media comprised of Neurobasal A (Life Tech), basic fibroblast growth factor (Stem Cell Tech) (20 ng/mL), epidermal growth factor (Sigma) (20 ng/mL), B27 without vitamin A (Life Tech), non-essential amino acids (Life Tech), Glutamax (Life Tech), sodium pyruvate (Life Tech), and penicillin/streptomycin (Life Tech).

Cells were plated on a Matrigel (Fisher) monolayer at a density of 600,000 cells in a 10 cm tissue culture dish, or in the absence of an extracellular matrix to promote tumorsphere formation. Differentiation of BTSCs was induced by culturing xenografts in 10% Fetal Bovine Serum (Atlanta Biologicals) in DMEM (Life Tech) with penicillin/streptomycin for at least 21 days.

Immunofluorescence

Coverglasses were coated with poly-D-lysine (PDL) (10 µg/mL, Sigma) followed by fibronectin (40 µg/mL, Sigma). Tumor cells were then plated onto the PDL/fibronectin coated coverglasses in stem cell media. After 2 days, cells were immunostained for specific antigens with primary antibodies at 5–10 µg/mL, and secondary antibodies at 2 µg/mL. CD133 (Miltenyi): Cells were live labeled for 10 min with anti-CD133 at 37 °C. This was followed by fixation with 2% paraformaldehyde, then incubation with an Alexa-488 antibodies secondary antibody (Life Tech). Nestin (Millipore), GFAP (Abcam), β3-tubulin (Abcam), O4 (Abcam): Cells were fixed with 4% paraformaldehyde, followed by blocking and permeabilization with 10% Normal Goat Serum (Jackson ImmunoResearch) and 0.1% Triton-X (Thermo Scientific). Cells were then labeled with primary antibodies for 1 h at room temperature, followed by secondary Alexa-488 antibodies. Nrp1 (Santa Cruz): Cells were fixed with 4% paraformaldehyde, followed by blocking and permeabilization with 10% Normal Donkey Serum (Jackson ImmunoResearch) and 0.1% Triton-X. Cells

were incubated with primary anti-Nrp1 overnight, followed by secondary Alexa-488 antibodies. A Zeiss Apotome microscope was used for imaging with a Zeiss AxioCam Mrm and Zeiss AxioVision software. Acquired images were then thresholded to controls to determine background fluorescence using Image J running on Java 6.

Animal housing

All mice were kept in a specific pathogen free (SPF) facility in accordance with Mayo clinic IACUC. Mice were kept in cages with circulating air and water and food ad libitum. Animals were monitored daily for signs of morbidity including but not limited to weight loss, tumor size, and decreased mobility.

Orthotopic tumor growth

BTSCs were dissociated, and stereotactically injected intracranially into athymic nude mice (Harlan), as previously described [57]. Briefly, cells were resuspended in dPBS at a density of 100,000 cells/mL for a total of 300,000 cells per mouse. Athymic nude mice were anesthetized with ketamine/xylazine, and placed into the stereotactic frame. A midline incision was made in the scalp, and a burr hole was made at specific coordinates using bregma as a landmark (1 mm anterior, 2 mm lateral, 3 mm deep). Using a Hamilton syringe, cell suspensions were injected at a rate of 1 µL per minute. The needle was slowly withdrawn, and incisions closed. Mice were given analgesics post-procedure, and monitored daily for signs of neurologic decline, at which point they were euthanized. Moribund mice were anesthetized with ketamine and xylazine, followed by perfusion with 0.1 M PBS and 4% paraformaldehyde (PFA). Brains were carefully removed and post-fixed overnight in 4% PFA, followed by cryoprotection in 30% sucrose. A cryostat was then used to cut 40- µm sections. Floating sections were rinsed in PBS, and permeabilized with 0.1% TritonX-100 and blocked with 10% NGS for 1 h. Overnight incubation of anti-human cytoplasmic antibody, STEM121 (Stem Cell Inc) was used to label tumor cells, followed by secondary Alexa-488 for 1 h. DAPI was used to label total nuclei.

TCGA data analysis

TCGA data analysis was performed using OncoLnc, an online tool that links TCGA mRNA/miRNA/lncRNA data with survival data. Genes of interest were queried and survival correlations were assessed comparing the top quartile of mRNA expression to the bottom quartile of mRNA expression. Statistical analysis was performed using a log-rank test [58].

PCR analysis

RNA was harvested from tumor cells using a Qiagen RNeasy kit and reverse transcribed (Select cDNA Synthesis Kit, BioRad). Amplicons were then transcribed from the cDNA by PCR using specific primer pairs (Platinum PCR, Life Tech). Products were then gel electrophoresed in 2% agarose DNA gels with ethidium bromide (BioRad). Bands were imaged using UV light (BioRad Gel Doc XR). 1 kb ladder (NEB) was used and primer detail with amplicon sizes included in Supp Fig. 8.

BrdU proliferation assay

BTSCs were dissociated from culture using gentle enzymatic dissociation (TrypLE) and plated on PDL/Fibronectin coated coverglasses at 10,000 cells per coverglass, and allowed to recover for 2 days. At this point, Time 0, the media was replaced with fresh stem cell media containing bromodeoxyuridine (BrdU) (Roche) with or without recombinant human Sema3A (R&D Systems). After 24 h, cells were fixed with 70% acidic ethanol for 20 min at -20 °C, followed by incubation with the primary anti-BrdU antibody (Roche), then secondary Alexa-488 and DAPI. Coverglasses were imaged using a Zeiss Apotome, imaging at least 13 representative fields per coverglass on an automated stage. BrdU and DAPI positive cells were then counted in ImageJ.

Cell death analysis

GBM Stem cells were plated at 10,000 cells per well onto PDL/Fibronectin coverglasses. Cells were treated as in the BrdU Proliferation Assays for 24 h. Next, plates were placed on ice and incubated with cold PI (Sigma) in stem cell media for 10 min. PI containing media was then removed and cells were fixed with 4% paraformaldehyde, followed by co-staining with DAPI for 1 h. Coverglasses were then imaged shortly thereafter using a Zeiss Apotome. PI and DAPI positive cells were then counted in ImageJ.

Gap migration assay

Gap migration assays were performed as previously described. Briefly, dissociated cells were plated onto PDL/Fibronectin coverglasses around a gap insert (Cell Bio Labs) at a density of 75,000 cells per well. After 48 h, inserts were removed and cell debris was washed away. Cells were then treated with Sema3A for 24 h, at which time coverglasses were fixed and stained with Alexa-488 conjugated phalloidin to label F-actin (Life Tech). Invasion was calculated based on percentage of positive cells in the previously cell free gap.

Tumorsphere invasion assay

Under sterile conditions, individual tumorspheres were carefully removed from culture and embedded into semi-solid Matrigel with or without Sema3A, in a low adhesion 96-well plate at a density of one tumorsphere per well. A layer of stem cell media was gently added with or without Sema3A, corresponding to Matrigel conditions. Initial tumorsphere diameters were measured using light microscopy and subsequent ImageJ analysis. After 24 h, tumorspheres were reimaged and changes in diameter were calculated.

shRNA Lentivirus production

Briefly, shRNA plasmids (Sigma) were obtained and transformed into competent *E. coli* bacteria by heat shock, and grown in liquid LB media in the presence of ampicillin at 37 °C. Glycerol stocks were made and frozen at -80 °C degrees for future use. Plasmids were then purified by Maxi Prep (Qiagen), and concentrations were determined using a spectrophotometer. 293 T cells were transfected with viral packaging plasmids, VSV-G, Gag, and Pol, in addition to the desired shRNA plasmid, using calcium chloride precipitation. Virions were collected in stem cell media minus growth factors, and stored at -80 °C for single use only. Titters were calculated by limiting dilution infection of 293 T cells, followed by puromycin selection. The number of colonies formed per condition was then calculated to determine the titer.

shRNA Lentivirus knockdown

Viral aliquots were thawed at room temperature, and added to cell cultures for an MOI of approximately 30. Viruses were incubated for 20–24 h. Viral media was then removed, and cells were washed three times with sterile PBS, and replaced with fresh stem cell media. After 4 days, cells were treated with puromycin to select for infected cells at a dose that kills 100% of uninfected cells within 2 days. Knockdown efficiency was determined by comparing mRNA expression between target and control shRNA samples. Briefly, cells were gently dissociated with TrypLE after selection, and mRNA was harvested and reverse transcribed. Specific primers were then used for qRT-PCR to compare gene expression between target and control samples, using the $\Delta\Delta Cq$ method, with actin serving as the housekeeping gene as previously described [59]. Constructs with the highest efficiency were selected for use. Virally infected stem cells were only maintained for a single passage to avoid extended culture of the tumor stem cells, and maintain consistent knockdown efficiencies across experiments.

In vivo flank tumor growth assay

Athymic nude-foxn1nu (NU/J) were ordered from Jackson Laboratories. Viral infected tumor cells were

harvested and injected into athymic nude mouse flanks at 400,000 cells or 1.2×10^6 cells per mouse according to standard protocol. Flank tumors were measured weekly by digital calipers to assess growth, with a final analysis at 7 weeks when tumors approached maximum IACUC approved size. Mice were euthanized using ketamine and xylazine, followed by perfusion with 0.1 M PBS and 4% paraformaldehyde (PFA). Tumors were then harvested for measurement of weight or cultured for re-analysis of expression to ensure maintenance of receptor knockdown.

Statistical analysis

Statistical analyses were performed using Graphpad Prism software (v7, San Diego, CA, USA). Normally distributed experimental results, as determined by the D'Agostino & Pearson omnibus test, were analyzed using the unpaired 2-tailed student's t-test for groups of 2, or one-way ANOVA with Bonferroni's post test for groups of more than 2. Mann Whitney test (groups of 2) or Kruskal-Wallis with Dunn's post test (> 2) were used for non-parametric results.

Results

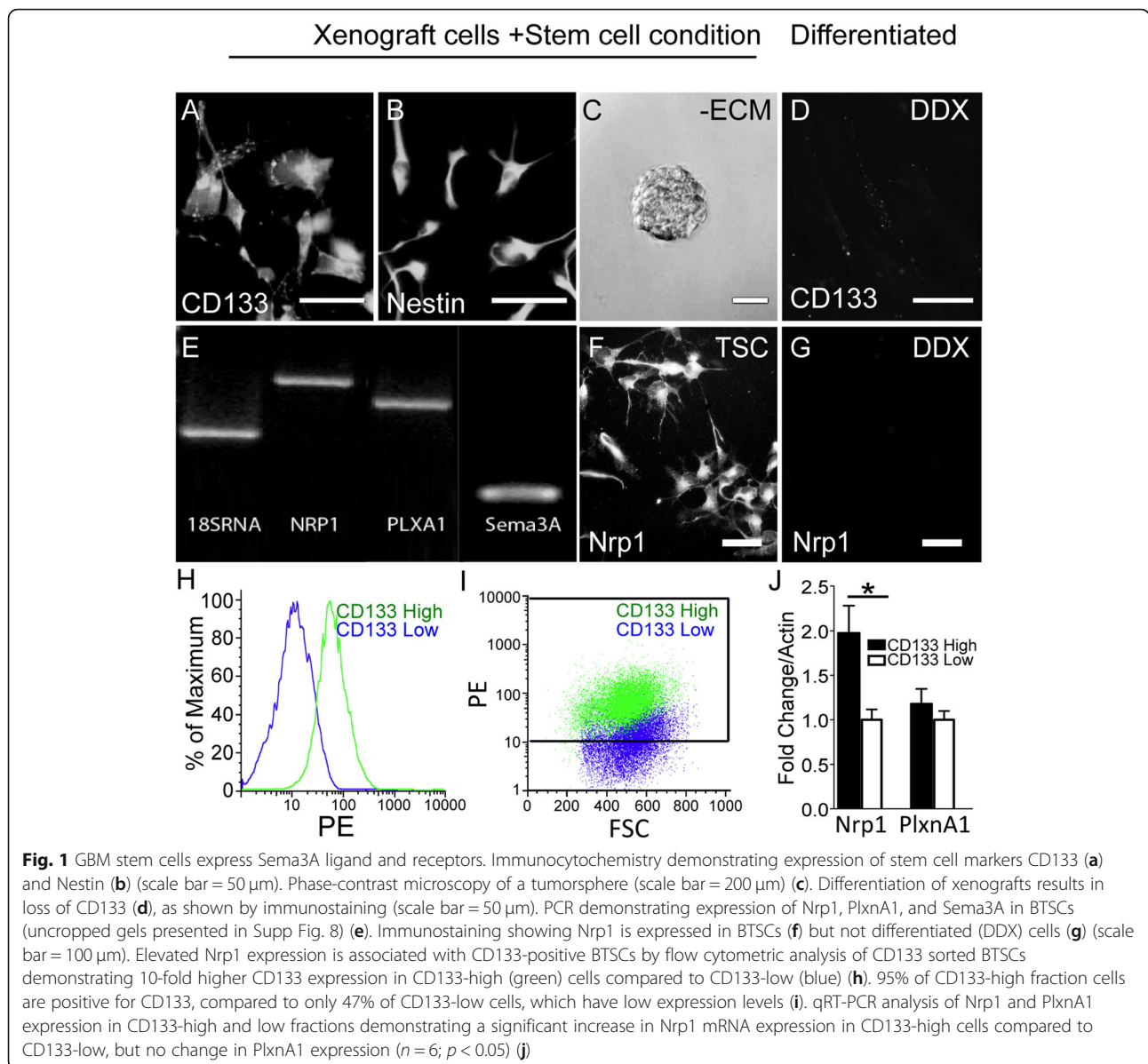
Glioblastoma stem cells express *Sema3A* ligand and receptors

We first identified the presence of BTSCs in isolated human xenograft cells cultured in stem cell conditions. Immunostaining confirmed prominent expression of the stem cell markers CD133 and Nestin (Fig. 1a,b) in the GBM6 line. When the xenograft cells were plated in stem cell conditions in the absence of extracellular matrix, self-adherent balls of tumor cells known as tumorspheres formed, indicating the presence of BTSCs (Fig. 1c). To test for multipotency, a hallmark of BTSCs, the GBM6 cells were assayed for ability to differentiate. Immunofluorescence microscopy revealed that upon differentiation in serum-containing media, the tumor cells downregulated CD133 expression (Fig. 1d) and upregulated markers of neural lineage positive cells including GFAP (astrocytes), $\beta 3$ tubulin (neurons), and O4 (oligodendrocytes) (Supp. Figure 1A-C). Differentiated GBM6 cells also lost the ability to form tumorspheres, and instead grew as a monolayer in the presence of serum-containing media (data not shown). When the BTSCs were injected intracranially into athymic nude mice, the implanted cells gave rise to highly invasive tumors (Supp. Figure 2). Importantly, due to the differences in growth rates of the KD tumors versus control tumors, orthotopic studies had technical limitations preventing survival comparison between these groups. Thus, the BTSCs express stem cell markers, are multipotent, and have intrinsic capacity to proliferate in vivo and invade brain parenchyma to form tumors.

We then tested for expression of *Sema3A* ligand and receptors. Analysis by PCR demonstrated mRNA expression of *Nrp1*, *PlxnA1*, and *Sema3A* in BTSCs isolated from 6 out of 6 independent human GBM xenograft lines (Fig. 1e; Supp. Figure 3). Of the lines tested, GBM6 is our most well characterized line with regard to maintenance of stem cell properties based on our previous work. As such, our functional experiments were performed using this xenograft line. Immunofluorescence staining showed high *Nrp1* expression in undifferentiated BTSCs (Fig. 1f). In contrast, the *Nrp1* immunostaining was lost in the tumor cells upon differentiation in serum-containing media (Fig. 1g, Supp. 1D). Downregulating *Nrp1* expression by lentiviral mediated shRNA knockdown (*Nrp1*-KD) also caused loss of *Nrp1* immunostaining, indicating specificity of the antibody (Supp. Figure 4). TCGA data correlating expression of these three transcripts (*Nrp1*, *PlxnA1*, *Sema3A*) with survival show that patients in the lower quartile of expression for all three markers live significantly longer than patients in the higher quartile of expression for both GBM and low-grade gliomas (Supp. Figure 5). A total of 152 GBM patients and 510 LGG patients with available mRNA data were included for this analysis. Taken together, these data show that GBM xenograft-derived multipotent BTSCs express *Sema3A* ligand and receptors, but *Nrp1* expression is lost upon differentiation.

CD133 positive cells highly express *Nrp1*

We next determined the proportion of CD133-positive cells comprising xenograft tumors, and the potential correlation with *Nrp1* expression. The xenograft tumor cells were labeled with CD133 antibodies conjugated to paramagnetic microbeads, and then sorted into high and low fractions using magnetic columns (bound vs. void volumes, respectively). Analysis by quantitative flow cytometry demonstrated a 10-fold increase in CD133 intensity in the high fraction (bound) compared to the CD133-low fraction (unbound; Fig. 1h). Also, 95% of the cells in the high fraction expressed CD133, compared to only 47% in the low fraction, and 62% in the unsorted cells (Fig. 1i). Analysis of mRNA isolated from the fractions by qRT-PCR showed that the CD133-high fraction demonstrated an approximately 2-fold increase in *Nrp1* expression compared to the CD133-low fraction (1.97 ± 0.31 vs. 1.00 ± 0.12 , respectively), but there was no significant difference in *PlxnA1* expression between the two groups (1.18 ± 0.17 vs. 1.00 ± 0.10 , respectively) (Fig. 1j). Thus, CD133-positive cells comprise a majority of the xenograft tumor and have elevated *Nrp1* expression compared to CD133-negative/low cells.

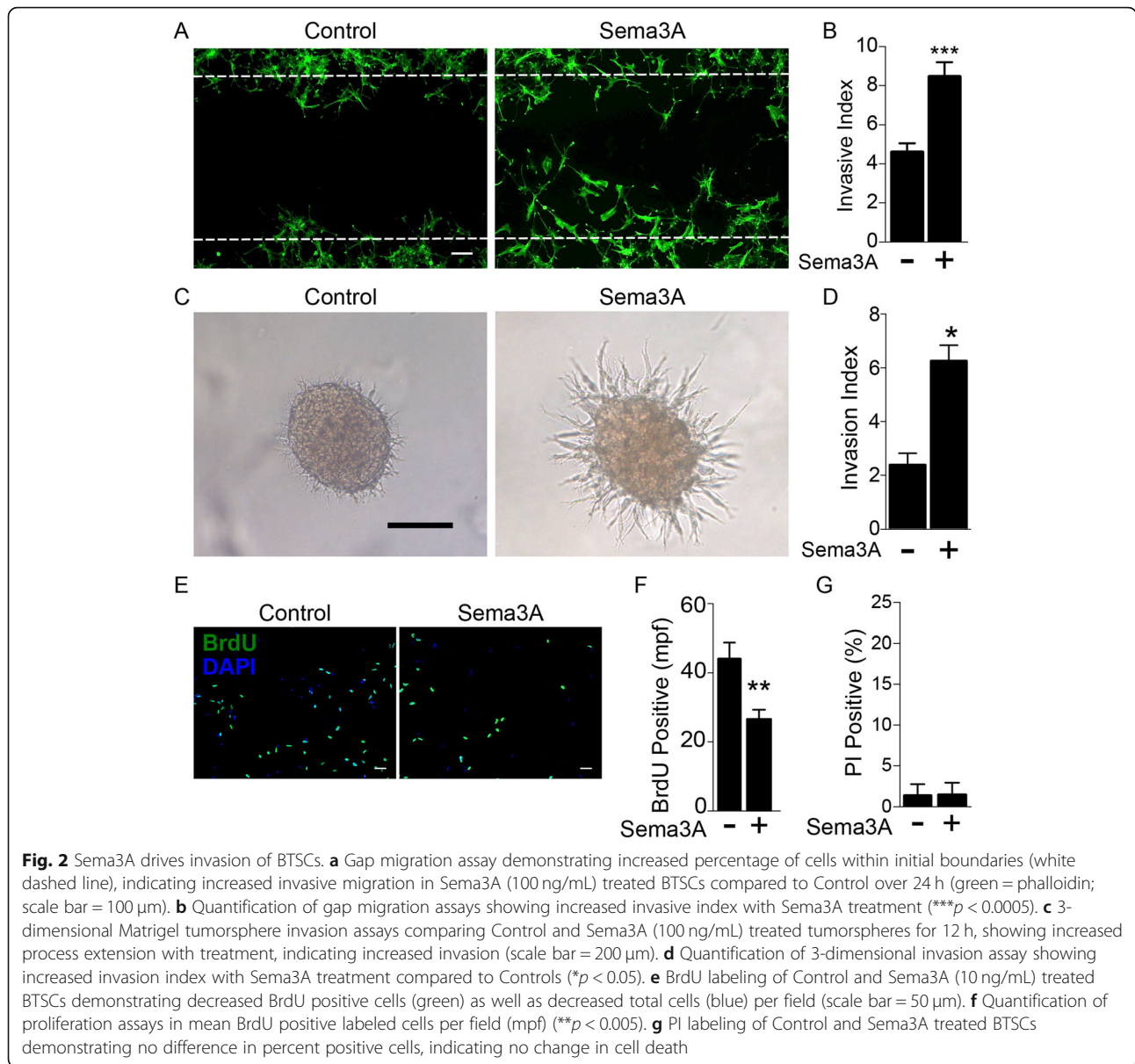


Sema3A drives BTSC invasion but inhibits proliferation

Because Semaphorin 3A is classically known for its role in cellular migration, we sought to determine whether or not it also regulated BTSC invasion. We utilized a quantitative cell migration assay whereby BTSCs are plated surrounding a protective stamp. The stamp is later removed to create a cell-free gap, and cell migration into the gap is measured. We found that BTSCs treated with Semaphorin 3A demonstrated a 2-fold increase in the number of cells occupying the gap compared to untreated BTSCs, indicating increased invasive migration ($8.5\% \pm 0.7$ vs. 4.6 ± 0.5) (Fig. 2a,b). Similarly, using a 3-dimensional invasion assay, we found that tumorspheres embedded in extracellular matrix (ECM) and treated with Semaphorin 3A demonstrated increased process extension

compared to control untreated tumorspheres, as determined by the mean change in tumorsphere diameter, and signifying increased invasion ($6.22\% \pm 0.59$ vs. $2.36\% \pm 0.43$) (Fig. 2c,d).

One plausible explanation for higher cell counts in the gap migration assay is a significant change in the rate of cell division, thereby causing an overall increase in cell numbers. Therefore, to assess the role of Semaphorin 3A in regulating BTSC proliferation, we labeled cells with BrdU in the presence or absence of exogenously applied Semaphorin 3A and quantified changes in BrdU uptake by immunofluorescence microscopy. Surprisingly, compared to untreated control cells, treatment with Semaphorin 3A resulted in a significant decrease in the mean number of BrdU-positive cells per field (43.94 ± 4.73 vs. $26.73 \pm$



2.72, respectively) (Fig. 2e,f). Staining for dead cells with PI in the BTSC culture showed no change in the percentage of positively labeled cells with Sema3A treatment, indicating no change in cell death (Fig. 2g). Taken together, these findings reveal that pro-migratory effects of Sema3A on BTSCs are associated with inhibition of cell proliferation, with no effect on cell death. To determine the effects of Sema3A on tumors of other backgrounds, we tested 3 additional BTSC lines (Supp Fig. 6). Sema3A treated GBM8, 38 and 39 showed decreased proliferation similar to GBM6, although GBM39 treatment resulted in statistically significant decreased proliferation at higher concentrations of Sema3A (GBM8: 0 ng/mL = 147.9 \pm 4.7; 10 ng/mL = 119.4 \pm 4.0, $p < 0.0001$; 100 ng/mL = 122.4 \pm 4.2, $p = 0.0001$); (GBM

38: 0 ng/mL = 83.0 \pm 5.603; 10 ng/mL = 69.19 \pm 3.63, $p = 0.04$; 100 ng/mL = 73.30 \pm 3.9, $p = 0.16$); (GBM 39: 0 ng/mL = 32.43 \pm 3.67; 10 ng/mL = 33 \pm 7.46, $p = 0.94$; 100 ng/mL = 21 \pm 2.74, $p = 0.014$). Cell cycle analysis in GBM6 cells demonstrated an increase in G0/G1 phase (Control - 58%, Sema3A treated - 82.8%) with decrease in G2/M (Control - 39%, Sema3A - 11.7%) in Sema3A treated cells compared to controls, without an increase in the sub-G0 fraction (Supp. Fig. 7).

Sema3A anti-proliferative effects require Nrp1

To further assess the role of Sema 3A in BTSC proliferation, we measured proliferation rates after downregulating Nrp1 and PlxnA1 expression by lentiviral-mediated shRNA knockdown (Nrp1-KD and PlxnA1-KD,

respectively). Analysis by qRT-PCR demonstrated knockdown efficiencies of greater than 80% relative to non-targeting virus (NT) infected BTSCs (NT-BTSCs) (Supp. Figure 4a). Decreased Nrp1 immunostaining in Nrp1-KD BTSCs compared to NT-BTSCs also indicated a corresponding decreased protein expression (Supp. Figure 4B).

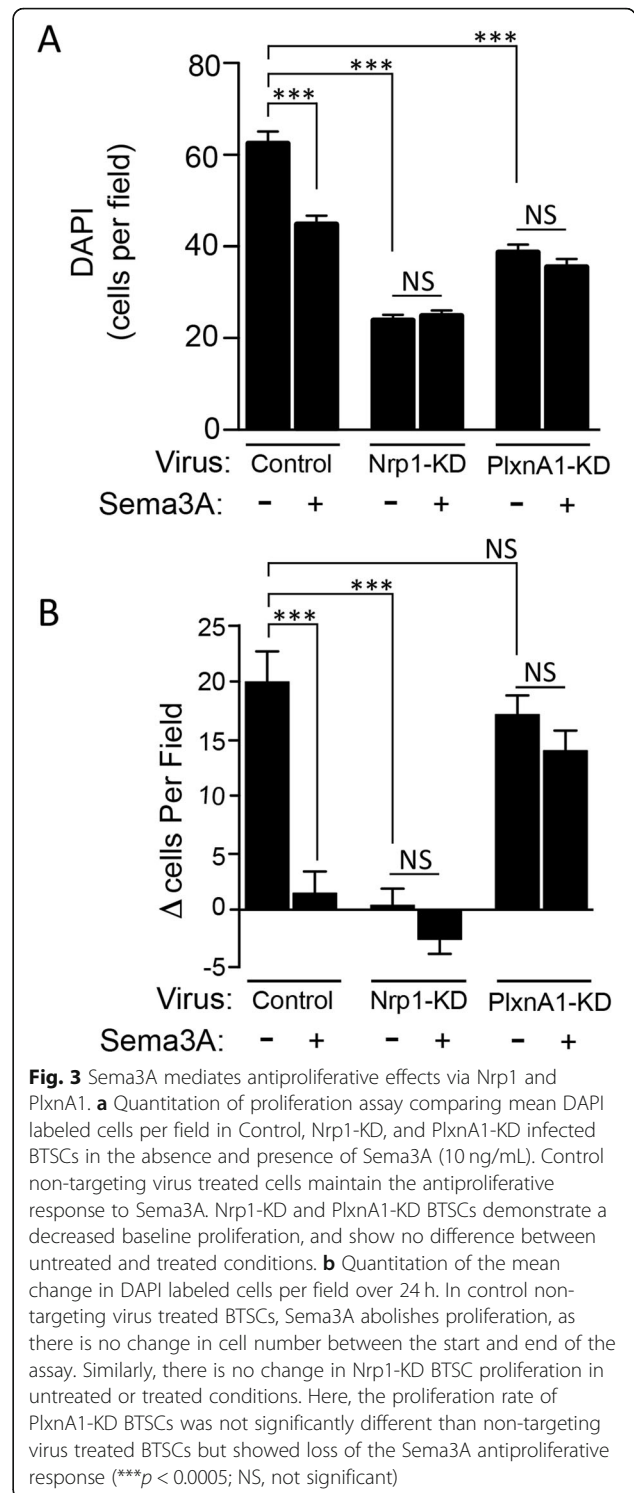
At baseline, Nrp1-KD and PlxnA1 -KD resulted in fewer cells per field compared to NT-BTSCs, as determined by a decrease in mean number of DAPI-stained cells per field (NT = 63.7 ± 2.7 ; Nrp1-KD = 23.8 ± 1.3 ; PlxnA1 -KD = 38.73 ± 1.8), indicating decreased proliferation (Fig. 3a). Treatment with SemA3A decreased proliferation of NT-BTSCs (45.5 ± 1.9), but showed no change in either Nrp1-KD or PlxnA1 -KD cells (24.8 ± 1.3 and 35.5 ± 1.8 , respectively). When comparing instead the mean change in cells per field during the treatment exposure, we found that SemA3A completely abolishes proliferation of NT-BTSCs over that time period (19.9 ± 2.7 vs. 1.4 ± 1.9) (Fig. 3b). Nrp1-KD had a baseline change in cells per field similar to that of control SemA3A treated cells (0.3 ± 1.5), and was unresponsive to SemA3A treatment (-2.7 ± 1.3) (Fig. 3b). The baseline change in PlxnA1-KD BTSCs, however, resembled that of untreated control cells (17.1 ± 1.7), but was also unresponsive to SemA3A (13.9 ± 1.8) (Fig. 3b).

Sema3A promotes migration via Nrp 1

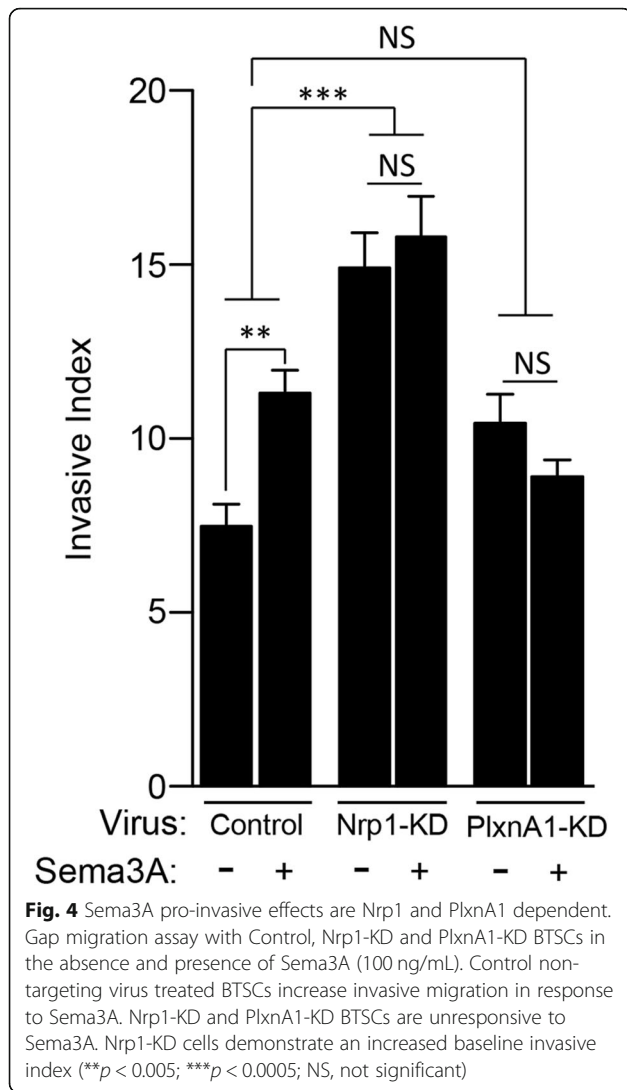
Using the gap migration assay, we confirmed that NT-BTSCs were stimulated to migrate in response to SemA3A (Ctrl = $7.5\% \pm 0.6$; SemA3A = $11.35\% \pm 3.9$) (Fig. 4). In contrast, Nrp1-KD BTSCs exhibited increased basal migration even without SemA3A treatment (Ctrl = $14.94\% \pm 1.0$; SemA3A = $15.83\% \pm 1.2$) (Fig. 4). Given that Nrp1 normally inhibits the intrinsic activity of its co-receptor, PlxnA1, we then measured the migration of PlxnA1-KD cells and found that their migration rates were within the range of NT-BTSCs. The PlxnA1-KD BTSCs also were unresponsive to SemA3A treatment. Taken together, these data suggest that SemA3A stimulates migration through the canonical Nrp1- PlxnA1 signaling module, and Nrp1-KD is sufficient to drive invasion.

Downregulation of Sema3A receptors inhibits GBM growth in vivo

Based on our findings that SemA3A and cognate receptors can regulate cell growth in cell-based assays, we then studied the effects of receptor knockdown on proliferation in vivo, injecting each NT, Nrp1-KD, and PlxnA1-KD BTSCs into the flank of athymic nude mice ($n = 5$ per group). Animals were randomized into the different experimental groups. Both Nrp1-KD and PlxnA1-KD demonstrated a slower rate of growth than NT-



BTSCs, as determined by changes in tumor diameter, though only Nrp1-KD reached statistical significance (Fig. 5a). At the endpoint of 7 weeks, mean tumor diameter of NT-BTSCs ($13.1 \text{ mm} \pm 2.4$) was greater than that of Nrp1-KD BTSCs ($0.0 \text{ mm} \pm 0.0$), and approached



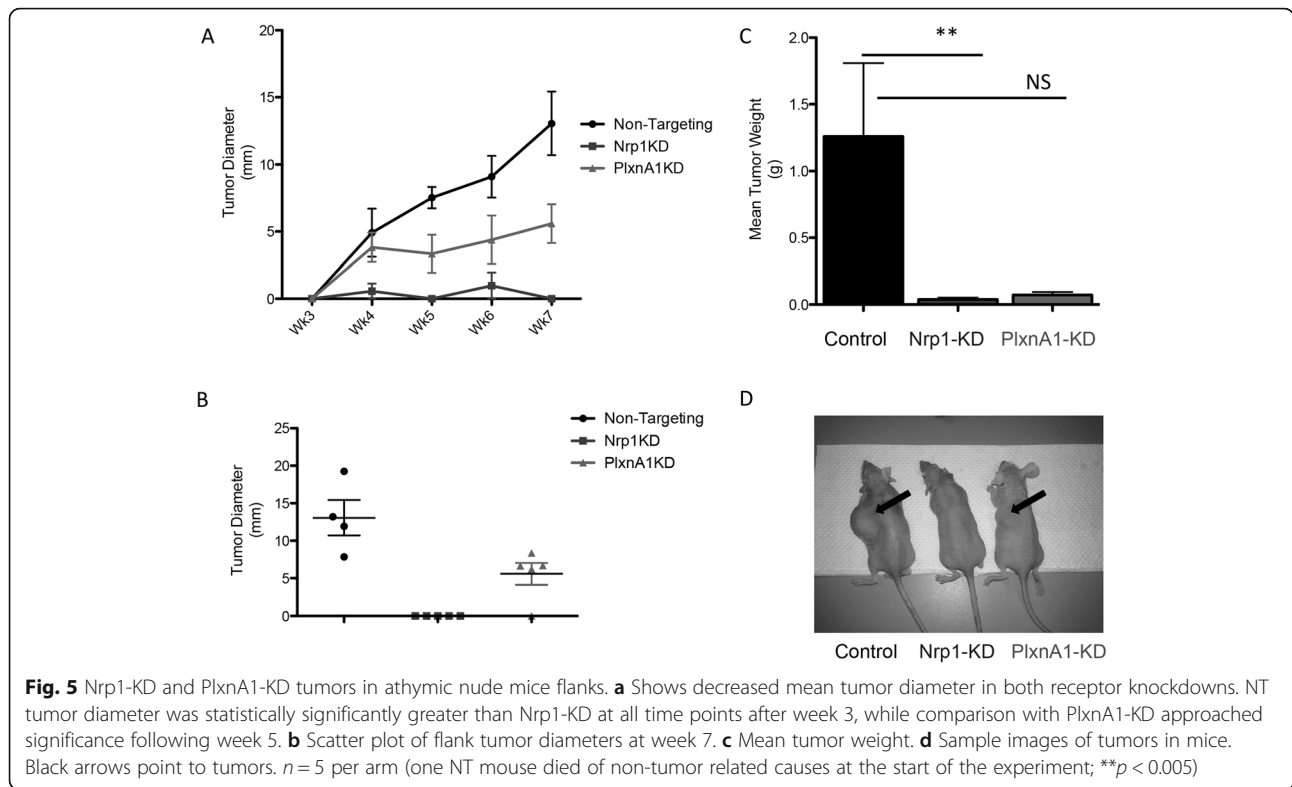
significance for PlxnA1-KD BTSCs (5.6 mm ± 1.4) (Fig. 5b). To address potential engraftment issues of KD cells, 3-fold more cells were injected into the flanks (1.2 × 10⁶ vs. 4.0 × 10⁵). These tumors were then excised and weighed to obtain final tumor volumes, as another metric of tumor growth. Consistent with our previous findings, NT-BTSCs were larger (1.26 g ± 0.5) when compared to Nrp1- KD (0.04 g ± 0.01 g) and PlxnA1-KD (0.07 g ± 0.02; not statistically significant) BTSCs (Fig. 5c,d). Finally, we examined TCGA survival data in both low grade glioma and glioblastoma based off expression levels of these three transcripts: Sema3A, Nrp1, PlxnA1. In all cases the lowest quartile of transcript expression survived significantly longer than the highest quartile of transcript expression. (Supp. Figure 5). Altogether, these data demonstrate that the Nrp1 receptor is a significant regulator of BTSCs and GBM tumor growth in vivo.

Discussion

Here, we demonstrate that treatment of BTSCs with Sema3A leads to inhibition of proliferation and stimulation of invasion in a Nrp1- and PlxnA1-dependent manner. Furthermore, decreased expression of Sema3A receptors is sufficient to inhibit proliferation and increase invasion.

Previous studies have found that Sema3A binding to Nrp1 results in disinhibition of PlxnA1, resulting in pathway activation [37]. We thus hypothesized that knockdown of Nrp1 expression should mimic Sema3A signaling, as PlxnA1 would then be more active. Conversely, knockdown of PlxnA1 should mimic a state in which there is no Sema3A ligand. Interestingly, we found that this was not the case. In GBM6 BTSCs, both Nrp1-KD and PlxnA1-KD mimicked Sema3A binding, showing decreased proliferation and increased invasion. In vivo, Nrp1-KD and PlxnA1-KD resulted in decreased proliferation, consistent with in vitro results. Based on these findings, it appears that in GBM, baseline Nrp1/PlxnA1 signaling provides a pro-proliferative signal to BTSCs, which is then inhibited by Sema3A binding and shifted toward an invasive signal. One possibility, given that Nrp1 is associated with BTSCs, is that Nrp1/PlxnA1 signaling promotes stemness, and inhibition of this pathway results in differentiation. Additional studies are therefore warranted to determine the exact mediators of Sema3A induced invasion. Downstream mediators of Sema3A signaling also warrant further investigation. Erk phosphorylation has been shown to mediate Sema3A-induced axon guidance [52]; yet in endothelial cells, Sema3A inhibits Erk phosphorylation and inhibits VEGF mediated proliferation [44]. Thus, Erk phosphorylation may be poised to provide a mechanistic switch between proliferative and invasive states for Sema3A signaling. Other potential mediators include Rac, which has been shown to be modulated by PlxnA1 signaling [53] but also is regulated by the cell cycle changes, in particular by the cell cycle inhibitor p27 [54].

The data presented here aimed to evaluate the effects of exogenous Sema3A on Nrp1 and PlxnA1, whereas prior research has focused mainly on autocrine Sema3A [53–55, 60]. Bagci et al. showed that U87 and A172 GBM cell lines express Nrp1, and are stimulated to invade in response to autocrine Sema3A treatment [55]. A subsequent study by Sabag et al., which also included U87 cells, reported that Sema3A inhibited proliferation in these cell lines, consistent with our findings [60]. However, neither study investigated the role of the receptor complex in Sema3A signaling, nor the effects in BTSCs. Functional blocking studies targeting Sema3A have also been utilized, highlighting the role of the pathway in tumor progression. Lee et al. showed that systemic administration of the Sema3A neutralization antibody, F11,



inhibited PDX GBM growth in a flank tumor model. The authors concluded that *Sema3A* inhibition was likely devascularizing the tumors, leading to decreased proliferation. In a follow-up study, the group also examined direct proliferation changes of GBM cell lines with inhibition of autocrine signaling [54]. The authors found that inhibiting autocrine *Sema3A* inhibited proliferation, suggesting that autocrine *Sema3A* was driving proliferation. However, neither the effects of direct receptor inhibition on proliferation nor that of exogenous *Sema3A* were examined. *Sema3A* is able to bind to non-canonical receptors, and our study presented here shows that inhibiting *Nrp1* abrogates proliferation, as does *PlxnA1* to lesser extent. The interplay between exogenous and autocrine *Sema3A* on signaling may be more complicated, and does require further examination. For instance, Treps et al. show that GBM promotes endothelial disruption by secreting *Sema3A* in extracellular vesicles and that these vesicles also signal in a *Nrp1* dependent fashion [61].

Our results demonstrate primarily the response of GBM6, an EGFR^{viii} tumor, in response to *Sema3A*. It is possible that tumors of different genetic backgrounds may affect responsiveness. Recent studies by Nasarre et al., found no effect on proliferation of *Sema3A* treatment in C6 rat glioma cells [62]. However, we have found that multiple GBM lines similarly respond to *Sema3A*, though required doses vary. This may be due to the

heterogenous backgrounds or changes in response to serial passaging. Rizzolio et al., demonstrated that EGFR served as a co-receptor for *Nrp1* in GBM cell lines, and EGFR internalization and signaling was dependent on *Nrp1* [63]. We have shown here that both wild type and viii EGFR BTSCs express *Nrp1* and *PlxnA1*. Similarly, BTSCs from the GBM6 line were immunosorted based on CD133 surface expression. The use of CD133 alone as a reliable BTSC marker has been controversial, as the CD133 protein is able to be truncated, glycosylated and endocytosed variably across glioma cells [7, 64]. For this reason, we confirmed the stemness of the isolated BTSCs through tumorsphere and differentiation assays that demonstrated a correlation between stemness and CD133 expression in our cells. Further studies addressing the potential interplay between EGFR and cognate *Sema3A* receptors in BTSCs are thus needed.

A long observed paradigm in cancer biology is that tumors that are highly proliferative tend to be less invasive, and vice versa, those that are highly invasive tend to be less proliferative, which has come to be known as the “go or grow” theory [16]. The ability to decrease the invasiveness of GBM could have profound effects on the efficacy of therapies, as previous studies have shown that more migratory cells tend to be less sensitive to chemotherapies. Our findings build upon previously published work by Jacob et al. that show high *PlxnA1* expression is associated with poorer overall survival in both TCGA

and Rembrandt GBM cohorts [52]. While previous studies have shown that Nrp1 is expressed in high and low grade glioma biopsies, our study is the first to show that higher expression of Nrp1, PlxnA1 and Sema3A are all associated with decreased survival in both GBM and LGG cohorts [65]. Although the median survival for Low grade glioma patients with low expression of Sema3A/Nrp1/PlxnA1 is significantly greater than those with high expression, the curves do converge at long-term endpoints. This is likely due to malignant transformation of low grade gliomas leading to a convergent phenotype. Additionally, a shift in the BTSC population from invasive to proliferative would potentially increase their sensitivity to chemotherapeutics that preferentially target dividing cells. The Sema3A pathway is therefore well poised to be a key regulator of BTSC responsiveness to treatment, and thus a promising therapeutic target [4, 66, 67]. Although our study examined the effects of Sema3A on Nrp1 and PlxnA1 signaling it is important to note that recent studies have highlighted the role of Nrp2 in mediating Sema3A chemo-attraction, especially in the setting of Nrp1 blockade [62]. Future studies delineating these mechanisms and the interplay of Nrp1 and Nrp2 in human GBM are needed.

The ability to identify BTSCs a priori has been of great interest, with a number of such markers being identified in the past decade [7, 10]. However, given the phenotypic and genetic variability of GBMs, a larger pool of stem cell markers is needed in order to cover the potential differences between tumors [4, 66, 67].

Conclusions

Our findings here demonstrate a positive association between Nrp1 and CD133 positive BTSCs, with differentiated cells lacking Nrp1. These data implicate Nrp1 as a potential marker of BTSCs. We also demonstrate that treatment of BTSCs with Sema3A leads to inhibition of proliferation and stimulation of invasion in a Nrp1- and PlxnA1- dependent manner. Orthotopic injections comparing knockdown cells and differentiated cells could provide further insight into this possible mechanism, and is one limitation of our study. It remains to be determined whether there is a functional role of Nrp1 in maintaining BTSC stemness and tumor formation ability, as it is possible that Nrp1 inhibition of proliferation is indeed mechanistically linked to preventing differentiation. Further studies are warranted to explore this interplay.

Supplementary Information

The online version contains supplementary material available at <https://doi.org/10.1186/s12885-020-07694-4>.

Additional file 1: Supp. Fig. 1. Differentiation of xenografts results in upregulation of lineage markers for GFAP (A), β 3-tubulin (B), and O4 (C),

with absent Nrp1 (D) as shown by immunostaining (scale bar = 50um A-C; 100um D).

Additional file 2: Supp. Fig. 2. BTSCs form invasive tumors in the brain. BTSCs injected into the brain of athymic nude mice formed highly invasive tumors, seen at low (A,B) and high power (C,D) magnification invading across the corpus callosum to the contralateral hemisphere with injection tract (B) and corpus callosum (C) marked by black and gray arrows, respectively. BTSCs also invade into surrounding brain parenchyma from the perimeter of the tumor mass with invading cells marked by white arrows at both low (B) and high (D) magnifications (green = BTSCs labeled with human specific marker STEM121; blue = DAPI labeling total nuclei).

Additional file 3: Supp. Fig. 3. PCR analysis of mRNA from several GBM xenograft lines, demonstrating expression of Nrp1, PlxnA1, and Sema3A in all lines tested. The genetic background of each is listed below. Black arrows indicate faint bands. (uncropped gels presented in Supp Fig. 8)

Additional file 4: Supp. Fig. 4. Successful knockdown of receptor expression. (A) qRT-PCR demonstrating successful knockdown of Nrp1 and PlxnA1 with respective shRNA lentiviruses compared to control non-targeting (CTRL) shRNA lentivirus treated BTSCs. Actin was used as a housekeeping gene. (B) Immunostaining demonstrating decreased Nrp1 protein expression in Nrp1-KD (Right) compared to control non-targeting infected BTSCs (Left) (green = Nrp1, blue = DAPI; scale bar = 10 μ m).

Additional file 5: Supp. Fig. 5. TCGA analysis of patient survival in both GBM and low-grade glioma (LGG) cohorts comparing the upper quartile and lower quartile of patients based on mRNA expression of each transcript. Statistical significance was assessed using a log-rank test (p -values: PlxnA1 LGG, 0.018 and GBM, 0.008; Nrp1 LGG, 0.069 and GBM, 0.074; Sema3A LGG, 0.0006 and GBM, 0.0511).

Additional file 6: Supp. Fig. 6. Sema3A exerts anti-proliferative effects across multiple tumor lines. Cells per field quantified for PDX lines (A) GBM 8, (B) GBM 38, (C) - GBM 39. * = $p < 0.05$, ** = $p < 0.01$, *** = $p < 0.001$, **** = $p < 0.0001$.

Additional file 7: Supp. Fig. 7. Flow cytometric cell cycle analysis of GBM6 stem cells comparing control (A) versus (B) Sema3A treated cells. (A) Control - 10,680 cells counted, G1 = 58%, %S = 3.1, %G2 = 37.8. (B) Sema3A treated - 7425 cells counted, G1 = 82.8%, %S = 7.62, G2 = 8.9%.

Additional file 8: Supp. Fig. 8. Uncropped gels corresponding to Fig. 1e (A) and Supp. Figure 3

Abbreviations

GBM: Glioblastoma; Nrp1: Neuropilin 1; PlxnA1: Plexin A1; Sema3A: Semaphorin 3A; BTSC: Brain tumor stem cell; TCGA: The Cancer Genome Atlas; shRNA: Short hairpin RNA; mRNA: Messenger RNA; qRT-PCR: Quantitative real time polymerase chain reaction; KD: Knockdown; VEGF: Vascular endothelial growth factor; PDX: Patient derived xenograft; HGG: High grade glioma; LGG: Low grade glioma

Acknowledgements

S.H.C. was supported as the Ty Louis Campbell St. Baldrick's Foundation Scholar, and Kathryn S.R. Lowry Endowed Chair in Neurosurgery. S.H.C. was also supported by kind gifts from Victoria and Rider McDowell Family Foundation.

Authors' contributions

J.N.S., D.M.O.H, B.D.M., F.B.M, J.R.H, S.H.C, I.L.W. conceived of the ideas for this experiment. D.M.O.H and M. C carried out all portions of the experiments listed. M.S. and B. C provided assistance with experimental and statistical portions of the manuscript. D.M.O.H, M.C. and P.S.U. wrote the manuscript with review and insight from S.H.C, I.L.W, J.N.S, F.B.M. and J.R.H. D.M.O.H, M.C., M.S., B.C. prepared all figures and supplementary figures. D.M.O.H and P.S.U. edited figures for publication. All authors reviewed the manuscript. The authors read and approved the final manuscript.

Funding

This project was supported by the Mayo Clinic College of Medicine Medical Scientist Training Program, the Mayo Clinic SPORE, and the National

Institutes of Health (NS67311), all of which provided funding for personnel and supplies that went toward design, collection and analysis of the data.

Availability of data and materials

All data generated or analyzed during this study are included in this published article [and its supplementary information files]. Raw files are not available currently due to intellectual property development.

Ethics approval and consent to participate

All animal studies were approved by the Mayo Clinic Institutional Animal Care and Use Committee. All experiments were performed in compliance with and according to guidelines by the National Institutes of Health (NIH, Bethesda, MD, USA) and the Mayo Clinic (Rochester, MN, USA) Institutional Review Board and Institutional Animal Care and Use Committee guidelines.

Consent for publication

Not applicable.

Competing interests

No authors have any conflicts of interest to disclose.

Author details

¹Mayo Clinic: College of Medicine, Rochester, MN 55905, USA. ²Department of Neurosurgery, Columbia University Medical Center, 710 W. 168th Street, New York, NY 10032, USA. ³Department of Neurologic Surgery, Mayo Clinic, Rochester, MN 55905, USA. ⁴Currently: Cancer Biology Program, University of Hawaii Cancer Center, University of Hawaii at Mānoa, Honolulu, HI 96813, USA. ⁵Department of Radiation Oncology, Mayo Clinic, Rochester, MN 55905, USA. ⁶Currently: Department of Neurosurgery, University of Kansas Medical Center, Kansas City, KS 66160, USA. ⁷Division of Pediatric Neurosurgery, Department of Neurosurgery, Huntsman Cancer Institute, University of Utah, Salt Lake City, UT 84113, USA. ⁸Institute for Stem Cell Biology and Regenerative Medicine and the Ludwig Cancer Center, Stanford University Medical Center, Stanford, CA 94305, USA.

Received: 15 June 2020 Accepted: 26 November 2020

Published online: 10 December 2020

References

- Greenberg MS. Handbook of neurosurgery. 7 th; 2006.
- Kleihues P, Louis DN, Scheithauer BW, Rorke LB, Reifenberger G, Burger PC, et al. The WHO classification of tumors of the nervous system. *J Neuropathol Exp Neurol.* 2002;61:215–25 discussion 226–9.
- Kumar V, Abbas AK, Fausto N, Aster JC. Robbins & Cotran Pathologic Basis of disease E-book. Elsevier Health Sciences; 2009.
- Lacroix M, Abi-Said D, Fournay DR, Gokaslan ZL, Shi W, DeMonte F, et al. A multivariate analysis of 416 patients with glioblastoma multiforme: prognosis, extent of resection, and survival. *J Neurosurg.* 2001;95:190–8.
- Stupp R, Mason WP, van den Bent MJ, Weller M, Fisher B, Taphoorn MJB, et al. Radiotherapy plus concomitant and adjuvant temozolomide for glioblastoma. *N Engl J Med.* 2005;352:987–96.
- Louis DN, Ohgaki H, Wiestler OD, Cavenee WK, Burger PC, Jouvet A, et al. The 2007 WHO classification of Tumours of the central nervous system. *Acta Neuropathol.* 2007;114:97–109. <https://doi.org/10.1007/s00401-007-0243-4>.
- Cheshier SH, Kalani MYS, Lim M, Ailles L, Huhn SL, Weissman IL. A neurosurgeon's guide to stem cells, cancer stem cells, and brain tumor stem cells. *Neurosurgery.* 2009;65:237–50. <https://doi.org/10.1227/01.neu.0000349921.14519.2a>.
- Reya T, Morrison SJ, Clarke MF, Weissman IL. Stem cells, cancer, and cancer stem cells. *Nature.* 2001;414:105–11.
- Singh SK, Clarke ID, Hide T, Dirks PB. Cancer stem cells in nervous system tumors. *Oncogene.* 2004;23:7267–73.
- Singh SK, Clarke ID, Terasaki M, Bonn VE, Hawkins C, Squire J, et al. Identification of a cancer stem cell in human brain tumors. *Cancer Res.* 2003;63:5821–8.
- Singh SK, Hawkins C, Clarke ID, Squire JA, Bayani J, Hide T, et al. Identification of human brain tumour initiating cells. *Nature.* 2004;432:396–401.
- Campos B, Wan F, Farhadi M, Ernst A, Zeppernick F, Tagscherer KE, et al. Differentiation therapy exerts antitumor effects on stem-like glioma cells. *Clin Cancer Res.* 2010;16:2715–28.
- Bao S, Wu Q, McLendon RE, Hao Y, Shi Q, Hjelmeland AB, et al. Glioma stem cells promote radioresistance by preferential activation of the DNA damage response. *Nature.* 2006;444:756–60.
- Binder DK, Berger MS. Proteases and the biology of glioma invasion. *J Neurooncol.* 2002;56:149–58.
- Bolteus AJ, Berens ME, Pilkington GJ. Migration and invasion in brain neoplasms. *Curr Neurol Neurosci Rep.* 2001;1:225–32.
- Giese A, Bjerkvig R, Berens ME, Westphal M. Cost of migration: invasion of malignant gliomas and implications for treatment. *J Clin Oncol.* 2003; 21:1624–36.
- Giese A, Laube B, Zapf S, Mangold U, Westphal M. Glioma cell adhesion and migration on human brain sections. *Anticancer Res.* 1998;18:2435–47.
- Dandy WE. Removal of right cerebral hemisphere for certain tumors with hemiplegia: preliminary report. *JAMA.* 1928;90:823–5.
- James GW. Removal of the right cerebral hemisphere for infiltrating glioma: report of a case. *JAMA.* 1933;101:823–6.
- Jafri NF, Clarke JL, Weinberg V, Barani IJ, Cha S. Relationship of glioblastoma multiforme to the subventricular zone is associated with survival. *Neuro-Oncology.* 2013;15:91–6.
- Matsukado Y, Maccarty CS, Kernohan JW. The growth of glioblastoma multiforme (astrocytomas, grades 3 and 4) in neurosurgical practice. *J Neurosurg.* 1961;18:636–44.
- Stummer W, Novotny A, Stepp H, Goetz C, Bise K, Reulen HJ. Fluorescence-guided resection of glioblastoma multiforme utilizing 5-ALA-induced porphyrins: a prospective study in 52 consecutive patients. *J Neurosurg.* 2000;93:1003–13.
- Zagzag D, Esencay M, Mendez O, Yee H, Smirnova I, Huang Y, et al. Hypoxia- and vascular endothelial growth factor-induced stromal cell-derived factor-1 α /CXCR4 expression in Glioblastomas. *Am J Pathol.* 2008; 173:545–60. <https://doi.org/10.2353/ajpath.2008.071197>.
- Zollinger R. Removal of left cerebral hemisphere: report of a case. *Arch Neuropsych.* 1935;34:1055–64.
- Scherer HJ. The forms of growth in gliomas and their practical significance. *Brain.* 1940; <https://academic.oup.com/brain/article-abstract/63/1/1/263743>.
- Zarco N, Norton E, Quiñones-Hinojosa A, Guerrero-Cázares H. Overlapping migratory mechanisms between neural progenitor cells and brain tumor stem cells. *Cell Mol Life Sci.* 2019;76:3553–70.
- Kolodkin AL, Matthes DJ, Goodman CS. The semaphorin genes encode a family of transmembrane and secreted growth cone guidance molecules. *Cell.* 1993;75:1389–99.
- Kolodkin AL, Matthes DJ, O'Connor TP, Patel NH, Admon A, Bentley D, et al. Fasciclin IV: sequence, expression, and function during growth cone guidance in the grasshopper embryo. *Neuron.* 1992;9:831–45.
- Luo Y, Raible D, Raper JA. Collapsin: a protein in brain that induces the collapse and paralysis of neuronal growth cones. *Cell.* 1993;75: 217–27.
- Messersmith EK, David Leonardo E, Shatz CJ, Tessier-Lavigne M, Goodman CS, Kolodkin AL. Semaphorin III can function as a selective chemorepellent to pattern sensory projections in the spinal cord. *Neuron.* 1995;14:949–59. [https://doi.org/10.1016/0896-6273\(95\)90333-x](https://doi.org/10.1016/0896-6273(95)90333-x).
- Tessier-Lavigne M, Goodman CS. The molecular biology of axon guidance. *Science.* 1996;274:1123–33.
- Gherardi E, Love CA, Esnouf RM, Jones EY. The sema domain. *Curr Opin Struct Biol.* 2004;14:669–78.
- Koppel AM, Feiner L, Kobayashi H, Raper JA. A 70 amino acid region within the semaphorin domain activates specific cellular response of semaphorin family members. *Neuron.* 1997;19:531–7.
- He Z, Tessier-Lavigne M. Neuropilin is a receptor for the axonal chemorepellent Semaphorin III. *Cell.* 1997;90:739–51.
- Kitsukawa T, Shimizu M, Sanbo M, Hirata T, Taniguchi M, Bekku Y, et al. Neuropilin–Semaphorin III/D-mediated Chemorepulsive signals play a crucial role in peripheral nerve projection in mice. *Neuron.* 1997;19:995–1005. [https://doi.org/10.1016/s0896-6273\(00\)80392-x](https://doi.org/10.1016/s0896-6273(00)80392-x).
- Kolodkin AL, Levengood DV, Rowe EG, Tai Y-T, Giger RJ, Ginty DD. Neuropilin is a Semaphorin III receptor. *Cell.* 1997;90:753–62. [https://doi.org/10.1016/s0092-8674\(00\)80535-8](https://doi.org/10.1016/s0092-8674(00)80535-8).
- Neufeld G, Kessler O. The semaphorins: versatile regulators of tumour progression and tumour angiogenesis. *Nat Rev Cancer.* 2008;8:632–45.
- Nakamura F, Goshima Y. Structural and functional relation of Neuropilins. *Neuropilin.* 2002;55–69. https://doi.org/10.1007/978-1-4615-0119-0_5.

39. Rohm B, Rahim B, Kleiber B, Hovatta I, Püschel AW. The semaphorin 3A receptor may directly regulate the activity of small GTPases. *FEBS Lett.* 2000; 486:68–72. [https://doi.org/10.1016/s0014-5793\(00\)02240-7](https://doi.org/10.1016/s0014-5793(00)02240-7).
40. Schmidt EF, Strittmatter SM. The CRMP family of proteins and their role in Sema3A signaling. In: *Advances in experimental medicine and biology*. p. 1–11. https://doi.org/10.1007/978-0-387-70956-7_1.
41. Winberg ML, Noordermeer JN, Tamagnone L, Comoglio PM, Spriggs MK, Tessier-Lavigne M, et al. Plexin a is a neuronal Semaphorin receptor that controls axon guidance. *Cell.* 1998;95:903–16. [https://doi.org/10.1016/s0092-8674\(00\)81715-8](https://doi.org/10.1016/s0092-8674(00)81715-8).
42. Tamagnone L, Artigiani S, Chen H, He Z, Ming G-L, Song H-J, et al. Plexins are a large family of receptors for Transmembrane, secreted, and GPI-anchored Semaphorins in vertebrates. *Cell.* 1999;99:71–80. [https://doi.org/10.1016/s0092-8674\(00\)80063-x](https://doi.org/10.1016/s0092-8674(00)80063-x).
43. Bagnard D, Vaillant C, Khuth S-T, Dufay N, Lohrum M, Püschel AW, et al. Semaphorin 3A–vascular endothelial growth Factor-165 balance mediates migration and apoptosis of neural progenitor cells by the recruitment of shared receptor. *J Neurosci.* 2001;21:3332–41. <https://doi.org/10.1523/jneurosci.21-10-03332.2001>.
44. Guttman-Raviv N, Shraga-Heled N, Varshavsky A, Guimaraes-Sternberg C, Kessler O, Neufeld G. Semaphorin-3A and semaphorin-3F work together to repel endothelial cells and to inhibit their survival by induction of apoptosis. *J Biol Chem.* 2007;282:26294–305.
45. Serini G, Valdemiri D, Zanivan S, Morterra G, Burkhardt C, Caccavari F, et al. Class 3 semaphorins control vascular morphogenesis by inhibiting integrin function. *Nature.* 2003;424:391–7. <https://doi.org/10.1038/nature01784>.
46. Neufeld G, Lange T, Varshavsky A, Kessler O. Semaphorin signaling in vascular and tumor biology. In: *Advances in experimental medicine and biology*. p. 118–31. https://doi.org/10.1007/978-0-387-70956-7_10.
47. Fan J, Raper JA. Localized collapsing cues can steer growth cones without inducing their full collapse. *Neuron.* 1995;14:263–74. [https://doi.org/10.1016/0896-6273\(95\)90284-8](https://doi.org/10.1016/0896-6273(95)90284-8).
48. Klostermann A, Lohrum M, Adams RH, Püschel AW. The Chemorepulsive activity of the axonal guidance signal Semaphorin D requires dimerization. *J Biol Chem.* 1998;273:7326–31. <https://doi.org/10.1074/jbc.273.13.7326>.
49. Polleux F, Morrow T, Ghosh A. Semaphorin 3A is a chemoattractant for cortical apical dendrites. *Nature.* 2000;404:567–73. <https://doi.org/10.1038/35007001>.
50. Püschel AW, Adams RH, Betz H. Murine semaphorin D/collapsin is a member of a diverse gene family and creates domains inhibitory for axonal extension. *Neuron.* 1995;14:941–8. [https://doi.org/10.1016/0896-6273\(95\)90332-1](https://doi.org/10.1016/0896-6273(95)90332-1).
51. Song H. Conversion of neuronal growth cone responses from repulsion to attraction by cyclic nucleotides. *Science.* 1998;281:1515–8. <https://doi.org/10.1126/science.281.5382.1515>.
52. Campbell DS, Holt CE. Apoptotic pathway and MAPKs differentially regulate chemotropic responses of retinal growth cones. *Neuron.* 2003;37:939–52.
53. Jacob L, Sawma P, Garnier N, Meyer LAT, Fritz J, Hussenet T, et al. Inhibition of PlexA1-mediated brain tumor growth and tumor-associated angiogenesis using a transmembrane domain targeting peptide. *Oncotarget.* 2016;7:57851–65.
54. McAllister SS, Becker-Hapak M, Pintucci G, Pagano M, Dowdy SF. Novel p27(kip1) C-terminal scatter domain mediates Rac-dependent cell migration independent of cell cycle arrest functions. *Mol Cell Biol.* 2003; 23:216–28.
55. Bagci T, Wu JK, Pfannl R, Ilag LL, Jay DG. Autocrine semaphorin 3A signaling promotes glioblastoma dispersal. *Oncogene.* 2009;28:3537–50. <https://doi.org/10.1038/onc.2009.204>.
56. Chen X, Zhang M, Gan H, Wang H, Lee J-H, Fang D, et al. A novel enhancer regulates MGMT expression and promotes temozolomide resistance in glioblastoma. *Nat Commun.* 2018;9:2949.
57. Carlson BL, Pokorny JL, Schroeder MA, Sarkaria JN. Establishment, maintenance and in vitro and in vivo applications of primary human glioblastoma multiforme (GBM) xenograft models for translational biology studies and drug discovery. *Curr Protoc Pharmacol.* 2011; Chapter 14:Unit 14.16.
58. Anaya J. OncoLnc: linking TCGA survival data to mRNAs, miRNAs, and lncRNAs. *PeerJ Comput Sci.* 2016;2:e67.
59. Higgins DM, Wang R, Milligan B, Schroeder M, Carlson B, Pokorny J, et al. Brain tumor stem cell multipotency correlates with nanog expression and extent of passaging in human glioblastoma xenografts. *Oncotarget.* 2013;4:792–801.
60. Sabag AD, Bode J, Fink D, Kigel B, Kugler W, Neufeld G. Semaphorin-3D and Semaphorin-3E inhibit the development of tumors from Glioblastoma cells implanted in the cortex of the brain. *PLoS One.* 2012;7:e42912. <https://doi.org/10.1371/journal.pone.0042912>.
61. Treps L, Edmond S, Harford-Wright E, Galan-Moya EM, Schmitt A, Azzi S, et al. Extracellular vesicle-transported Semaphorin3A promotes vascular permeability in glioblastoma. *Oncogene.* 2016;35:2615–23.
62. Nasarre C, Koncina E, Labourdette G, Cremel G, Roussel G, Aunis D, et al. Neuropilin-2 acts as a modulator of Sema3A-dependent glioma cell migration. *Cell Adh Migr.* 2009;3:383–9. <https://doi.org/10.4161/cam.3.4.9934>.
63. Rizzolio S, Rabinowicz N, Rainero E, Lanzetti L, Serini G, Norman J, et al. Neuropilin-1-dependent regulation of EGF-receptor signaling. *Cancer Res.* 2012;72:5801–11. <https://doi.org/10.1158/0008-5472.can-12-0995>.
64. Barkeer S, Chugh S, Batra SK, Ponnusamy MP. Glycosylation of cancer stem cells: function in Stemness, tumorigenesis, and metastasis. *Neoplasia.* 2018; 20:813–25.
65. Frankel P, Pellet-Mary C, Lehtolainen P, D'Abaco GM, Tickner ML, Cheng L, et al. Chondroitin sulphate-modified neuropilin 1 is expressed in human tumour cells and modulates 3D invasion in the U87MG human glioblastoma cell line through a p130Cas-mediated pathway. *EMBO Rep.* 2008;9:983–9.
66. Colman H, Zhang L, Sulman EP, McDonald JM, Shooshtari NL, Rivera A, et al. A multigene predictor of outcome in glioblastoma. *Neuro-Oncology.* 2010; 12:49–57. <https://doi.org/10.1093/neuonc/nop007>.
67. Network TCGAR, The Cancer Genome Atlas Research Network. Comprehensive genomic characterization defines human glioblastoma genes and core pathways. *Nature.* 2008;455:1061–8. <https://doi.org/10.1038/nature07385>.

Publisher's Note

Springer Nature remains neutral with regard to jurisdictional claims in published maps and institutional affiliations.

Ready to submit your research? Choose BMC and benefit from:

- fast, convenient online submission
- thorough peer review by experienced researchers in your field
- rapid publication on acceptance
- support for research data, including large and complex data types
- gold Open Access which fosters wider collaboration and increased citations
- maximum visibility for your research: over 100M website views per year

At BMC, research is always in progress.

Learn more biomedcentral.com/submissions

